Quantitatively study on influencing factors of high multiple water flooding based on NMR technology

Jitao WANG[1], Junjian LI[1*]

1 College of Petroleum Engineering, China University of Petroleum(Beijing), Beijing 102249, China;
(15727310366@163.com)

ABSTRACT

With the development of oil field water flooding, many oil fields have entered the high water cut stage one after another, and some parts of the actual reservoir have been washed by water drive for many years, so the understanding of traditional oil drive efficiency needs to be improved, and the oil drive efficiency under high multiple displacement needs to be clarified. There are many factors affecting oil displacement efficiency. This paper mainly considers the influence of water displacement PV number, crude oil viscosity, permeability and water displacement velocity (capillary number). In order to reveal the changes of high-power water flooding from macroscopic and microscopic points of view, 21 sets of unsteady water flooding core experiments with water flooding PV number of 1000PV were carried out. Among them, 11 sets were high-power water flooding and measured parameters to calculate high-power phase permeability curves. The other 10 groups were subjected to NMR scanning during high-power water flooding to determine the effects of different permeability, viscosity and water flooding speed on the residual oil utilization of different pore sizes. The right shift ratio of residual oil and the expansion ratio of water phase permeability were selected to characterize the change law of high phase permeability.

The results show that the oil displacement efficiency increases with the increase of water displacement multiple, and the increase of oil displacement efficiency decreases with the increase of water displacement multiple. The oil phases in different pore radius are used, and the displacement efficiency of large holes is higher than that of small holes. With the increase of oil viscosity, the right shift ratio of residual oil in high-power water drive increases, which is 1.11 at low viscosity and 1.29 at high viscosity. With the increase of oil viscosity, the expansion ratio of water phase in high multiple water flooding increases, which is 1.07 at low viscosity and 2.28 at high viscosity. The higher the oil viscosity, the higher the oil potential is in high multiple water flooding. The increment of oil displacement efficiency in the low-viscosity group mainly comes from the large pores with pore radius greater than 20um, and the increment of oil displacement efficiency in the medium-high viscosity group mainly comes from the small pores with pore radius less than 10um. With the increase of core permeability, the right shift ratio of residual oil and the expansion ratio of water phase infiltration decrease, and the lower the permeability, the higher the oil increase potential of high multiple water flooding. The oil displacement efficiency of each pore radius in the low permeability group increased, and the increment of oil displacement efficiency in the high permeability group mainly came from the small hole about 8.62um. After high multiple water flooding, the right shift ratio of residual oil increases with the increase of capillary number, and the oil displacement efficiency is greatly improved at high speed, and the expansion ratio of water phase infiltration increases with the increase of capillary number after high multiple water flooding. High-speed water flooding can improve the water phase flow capacity, and the oil increase potential is lower at low speed. At low speed, the displacement efficiency of each aperture increases, and the increment of small aperture is more for 8.62um. The increment of displacement efficiency under high speed condition mainly comes from the large and medium aperture of 27.75um.

Keywords: high multiple water flooding, oil displacement efficiency, NMR scanning

NONMENCLATURE

Abbreviations	
PV	Pore volume multiple, dimensionless

Symbols	
$f_o(S_w)$	Oil content, dimensionless
$\bar{V}_o(t)$	Dimensionless cumulative oil production, dimensionless
$\bar{V}(t)$	Dimensionless cumulative fluid production, dimensionless
K_{ro}	Oil phase relative permeability, dimensionless
K_{rw}	Water phase relative permeability
I	Relative injection capacity, dimensionless
$Q(t)$	Liquid production flow at the end face of the outlet of rock sample at time t, cm^3/s
Q_o	Oil production at the outlet end face of rock sample at initial time, cm^3/s
Δp_o	Initial drive pressure difference, MPa

1. INTRODUCTION

At present, water flooding has become the main development mode of various oilfields. With the development of water flooding in onshore oilfields in China, various oilfields have successively entered the stage of high water cut. After years of water flooding in some parts of actual reservoirs, the understanding of traditional oil displacement efficiency needs to be improved, and the oil displacement efficiency under high multiple displacement needs to be clarified.

Water drive reservoir still has the potential to tap remaining oil after it enters the ultra-high water cut stage, but due to the influence of geological factors and development factors, the reservoir physical properties and the distribution of remaining oil are complicated. When multiphase fluid flows through porous media, the relative permeability can be used as a specific form of seepage characteristics. Xu J et al. found that the phase permeability curve is affected not only by the fluid properties and distribution characteristics inside the core, but also by various core properties. On the premise of fractal theory, Miao Tongjun et al. presented an analytical model of permeability and relative permeability considering the percolation characteristics of drip-slug flow in a capillary bundle, which was presented as a function of the microstructure parameters and fluid properties of porous media, and analyzed the percolation characteristics of drip-slug flow in fractal porous media. The influence of each parameter on the infiltration is studied and compared with the existing experimental results, the accuracy of the

expression is verified. In the oil-water two-phase flow, the viscosity ratio of oil to water has a great influence on the flow state, and the viscosity ratio of oil to water has an important influence on the shape of the phase permeability curve. Esmaeili S et al. found that the viscosity of crude oil and water is greatly affected by temperature, and Krause M H et al. found that the ratio of different oil phase and water phase viscosity has an important impact on the morphological characteristics of the relative permeability curve of the two phases. Especially for the heavy oil reservoir, the change of crude oil viscosity due to the change of temperature will have a great impact on the oil-water seepage state. In view of the influence of crude oil viscosity on the phase permeability curve, most predecessors adopted two approaches: The first one was to test the phase permeability curve with oil with unequal viscosity under the same experimental scheme; Another method is to test the relative permeability curve of the same crude oil at different temperatures. Reservoir is the carrier of fluid flow. Lai B et al. found that the complexity of reservoir space and surface wetting conditions directly affect the flow characteristics of internal fluids. Especially in the late period of ultra-high water cut, the physical properties of porous media in the reservoir have changed obviously due to the long-term erosion of injected water. In view of the analysis of the influence of reservoir properties on the phase permeability curve, Ge Y et al. conducted research by core displacement experiment method, Zhang D et al. by digital core simulation method, and Aghabozorgi S et al. by analytical calculation method.

With the deepening of the study of conventional seepage, many scholars have turned their attention to the study of high-power water flooding seepage. CHEN Ke et al. carried out a study on the mechanism of enhanced oil recovery by high-power water flooding through CT scanning imaging displacement technology, and found that after 2000PV water flooding, the oil displacement efficiency can be increased by 31.5% compared with conventional flooding. SUN Changwei et al. introduced the characteristics of high-power water flooding infiltration into numerical simulation to improve the accuracy of numerical simulation. Based on indoor displacement experiment and nuclear magnetic scanning, this paper will consider the effects of water displacement multiple, crude oil viscosity, permeability and water displacement velocity (capillary number) on high-power phase permeability, reveal the change law of high-power water displacement from macro and micro

perspectives, and provide some understanding for field development.

2. MATERIAL AND METHODS

The displacement water used in this experiment was manganese chloride solution with a concentration of 10000mg/L. The viscosity of simulated oil from low to high is 3# white oil, 26# white oil, 100# white oil, 250# white oil and 500# white oil, and the viscosity measured in laboratory is 2.0mPa·s, 25.0mPa·s, 95.0mPa·s, 264.0mPa·s and 502.0mPa·s, respectively. The cores used in the experiment are artificial cores with permeability ranging from about 50 to about 1700.

In this experiment, the unsteady method of oil-water relative permeability was adopted in the test method for two phase relative permeability in rock, National standard GB/T28912-2012. The unsteady oil-water relative permeability method is based on Buckley-Leverett one-dimensional two-phase water flooding front advance theory. Ignoring capillary pressure and gravity, assuming that the two-phase fluid is not miscible and incompressible, the saturation of oil and water in any cross-section of the rock sample is uniform. Instead of injecting two fluids into the core at the same time, the core is saturated with one fluid and displaced with the other. In the process of water flooding, the distribution of oil-water saturation in porous media is a function of distance and time, which is called an unstable process. According to the requirements of simulation conditions, constant pressure difference or constant velocity water displacement experiments are carried out on reservoir rock samples. The output of each fluid and the change of pressure difference at both ends of the rock samples with time are recorded at the outlet of the rock samples. The oil-water relative permeability is calculated by using the "JBN" method, and the relation curve between oil-water relative permeability and water saturation is plotted.

In order to reveal the change law of different water drive multiple, crude oil viscosity, permeability and water drive velocity during high-power water drive from macroscopic and microscopic perspectives, 21 sets of water drive core experiments with water-drive PV number of 1000PV were conducted by unsteady state method, as shown in Table.1 : Groups 1-11 were high-power water drive and measured parameters to calculate high-power phase permeability curve; In group 12-21, NMR scanning was performed during high-power water flooding to determine the effects of different permeability, viscosity and water flooding velocity on the residual oil utilization of different pore sizes. The right

shift ratio of residual oil and the expansion ratio of water phase permeability were selected to characterize the change law of high phase permeability.

Table.1 Experimental design parameters table

Experiment number	Permeability （mD）	Oil viscosity （mPa·s）	Displacement velocity （mL/min）
1	1477	2	0.1
2	1760	25	0.1
3	1640	95	0.1
4	1300	502	0.1
5	48	2	0.1
6	492	2	0.1
7	1218	2	0.1
8	1668	2	0.1
9	504	2	0.05
10	528	2	0.5
11	531	2	1.0
12	464	2	0.5
13	510	25	0.5
14	483	264	0.5
15	506	543	0.5
16	106	2	0.5
17	277	2	0.5
18	751	2	0.5
19	502	2	0.1
20	474	2	1.0
21	492	2	2.0

Experimental steps: (1) Core dry weight, vacuum for 2h after saturated water, wet weight to calculate the pore volume; (2) According to the simulated oil required by the experiment, using the simulated oil to flood water under constant pressure, the saturation of the generated bound water is about 35%; (3) According to the experimental conditions, select the appropriate water drive speed for displacement, accurately record the water breakthrough time, the cumulative oil production during water breakthrough, the cumulative liquid production, the water drive speed and the displacement pressure difference at both ends of the rock sample, and stop when the displacement reaches 1000 times the pore volume. Among them, group 1-11 is directly displaced to 1000 times the pore volume without removing the core, which can make the measurement more accurate. Groups 12-21 were scanned by indoor nuclear magnetic device when the water drive pore volume multiples were 50, 100, 500 and 1000, respectively.

3. THEORY AND CALCULATION

3.1 Calculation of oil-water relative permeability and water saturation by unsteady state method

In the process of water flooding, the oil content can be expressed as

$$f_o(S_w) = \frac{d\overline{V_o}(t)}{d\overline{V}(t)} \qquad (1)$$

The water saturation at the outlet of the sample can be expressed as

$$S_{we} = S_{ws} + \overline{V_o}(t) - \overline{V}(t)f_o(S_W) \qquad (2)$$

The relative injection capacity can be expressed as

$$I = \frac{Q(t)}{Q_o}\frac{\Delta p_o}{\Delta p(t)} \qquad (3)$$

Then the relative permeability of oil phase can be obtained

$$K_{ro} = f_o(S_w)\frac{d[1/\overline{V}(t)]}{d[1/I\overline{V}(t)]} \qquad (4)$$

The relative permeability of water phase can be expressed as

$$K_{rw} = K_{ro}\frac{\mu_w}{\mu_o}\frac{1-f_o(S_w)}{f_o(S_w)} \qquad (5)$$

3.2 Calculation of relative permeability evaluation index of high multiple water flooding

The relative permeability evaluation index of high-multiple water flooding is selected as the right-hand shift ratio of residual oil saturation (S_{orR}) and the expansion ratio of water phase relative permeability corresponding to residual oil saturation (K_{rwE}) when water flooding with 1000 pore multiple compared with water flooding with 50 pore multiple. The specific calculation parameters are shown as follows:

$$S_{orR} = \frac{S_{or_{1000PV}}}{S_{or_{50PV}}} \qquad (6)$$

$$K_{rwE} = \frac{K_{rw_{1000PV}}}{K_{rw_{50PV}}} \qquad (7)$$

4. RESULTS AND DISCUSSION

4.1 The effect of water flooding multiples

With the increase of water flooding multiple, the change reflected in the phase permeability curve is the right shift of residual oil saturation, and the resulting impact is the increase of oil displacement efficiency, as shown in Fig.1. By calculating the oil displacement efficiency of groups 1-11, it can be seen that the oil displacement efficiency of each group increases with the increase of water flooding multiple. By calculating the average value of each group, The average displacement efficiency increased from 60.78% at 50PV to 80.61% at 1000PV, with an increment of 19.84%.By calculating the

oil displacement efficiency increment with different water flooding multiples, it can be found in Fig.2 that the oil displacement efficiency increment decreases with the increase of water flooding multiples, the average increment of 1PV in the first 50PV is 0.09%, and only 0.01% in the last 500PV.
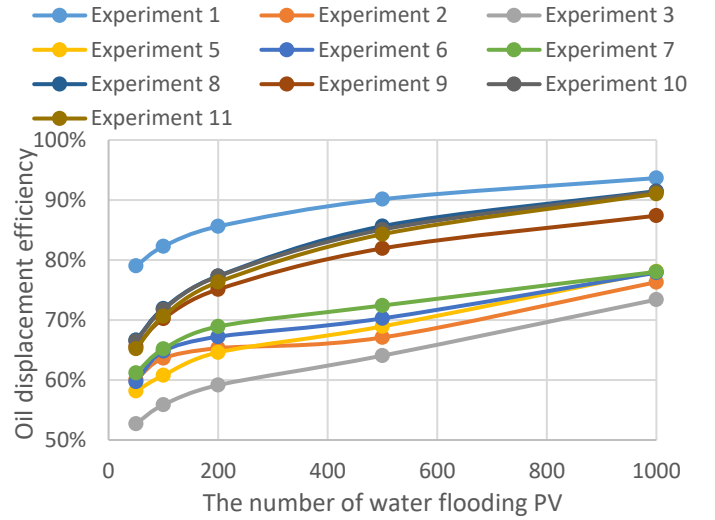

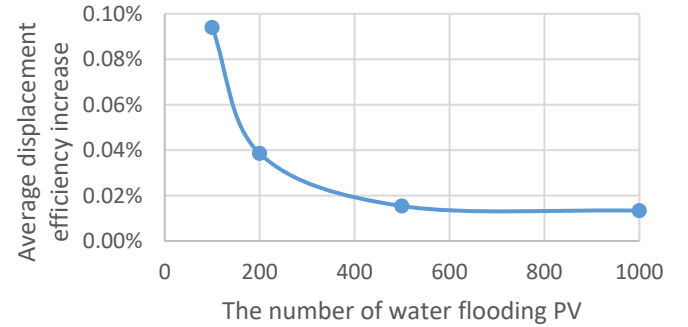Fig. 1 Group 1-11 oil displacement efficiency- the number of water flooding PV curve

Fig. 2 Group 1-11 average displacement efficiency increase- the number of water flooding PV curve

Taking the results of the 12th group of nuclear magnetic scans as an example, as shown in Fig.3, the oil displacement efficiency is calculated inversely based on the signal intensity area. According to the conversion relationship between pore size and T2 signal, r=CT2, and C value is 40, the oil displacement efficiency changes of each pore radius can be obtained under different displacement multiple. As shown in Fig.4, it can be found that core oil displacement efficiency increases with the increase of water drive PV number. From 66.62% to 74.8%, a total increase of 8.18%; By calculating the changes of oil confidence signs in different pore radii, it can be found, as shown in Fig.5, that the oil phases in different pore radii are used, and the oil displacement

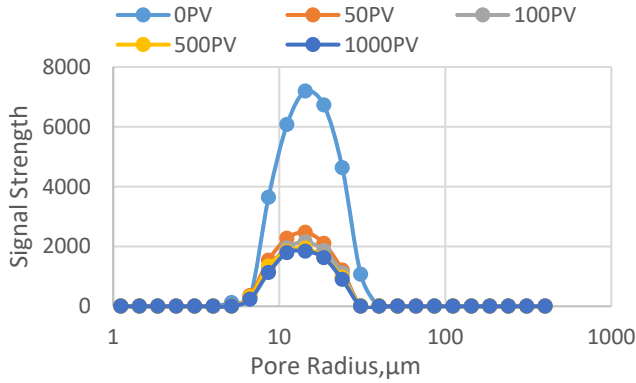efficiency of large holes in the basic group is higher than that of small holes.

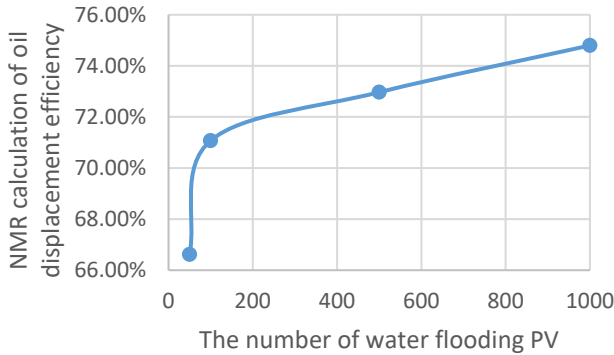Fig. 3 Experiment 12 Signal Strength- Pore Radius Curve

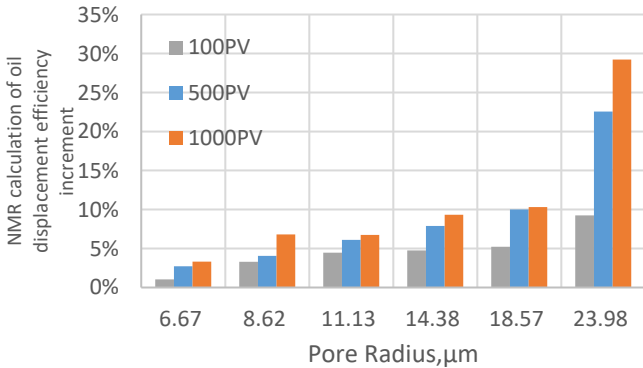Fig. 4 NMR calculation of oil displacement efficiency- The number of water flooding PV Curve

Fig. 5 NMR calculation of oil displacement efficiency increment- Pore Radius Curve

4.2 The effect of oil viscosity

By calculating the high multiple water flooding relative permeability curve of group 1-4, as shown in Fig.6, it can be found that as the viscosity of crude oil increases, the isotonic point shifts to the left, and the wettability gradually changes from water-wet to oil-wet. With the increase of crude oil viscosity, the residual oil saturation increases.
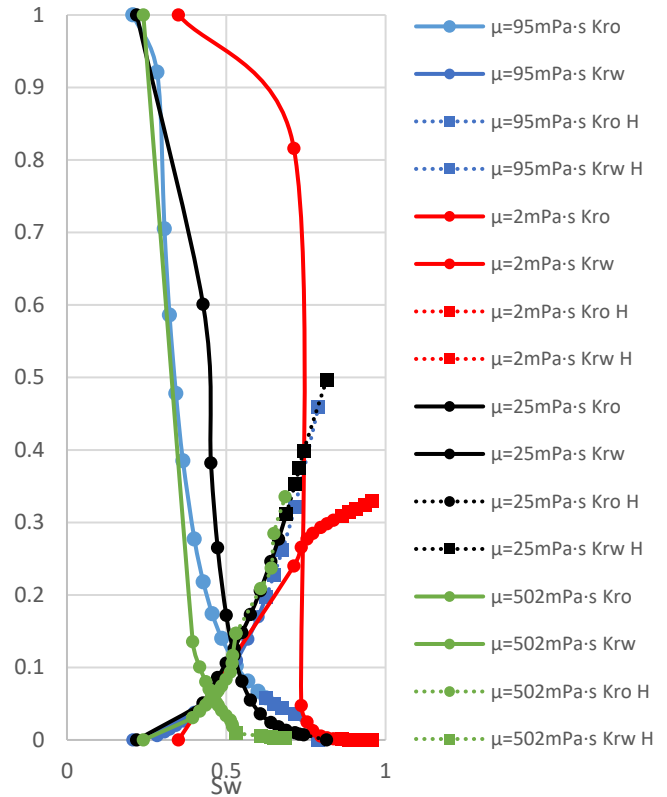
Fig. 6 Group 1-4 relative permeability curves of conventional and high-multiple water flooding with different viscosities

By comparing the right shift ratio of residual oil and the expansion ratio of water phase infiltration when the water drive ratio is 1000PV and 50PV, as shown in Fig.7 and Fig.8, it can be found that with the increase of crude oil viscosity, the right shift ratio of residual oil in high water drive increases, reaching 1.11 at low viscosity and 1.29 at high viscosity. With the increase of crude oil viscosity, the expansion ratio of water phase infiltration increases with high water flooding, which is 1.07 at low viscosity and 2.28 at high viscosity. It shows that the higher the viscosity of crude oil, the more potential of oil increase through high water flooding
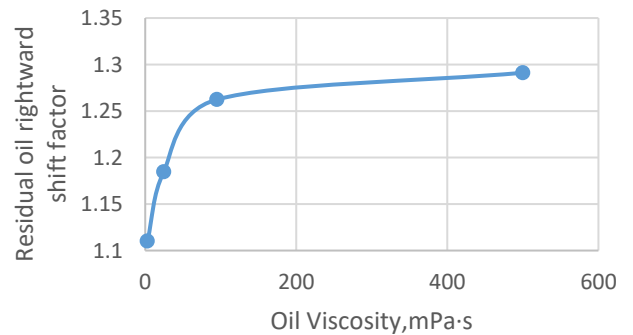

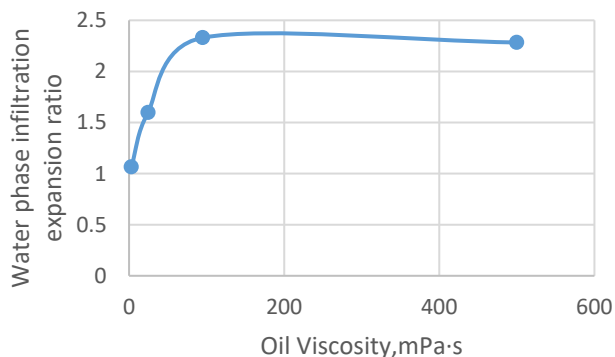Fig. 7 Residual oil rightward shift factor- Oil Viscosity Curve

Fig. 8 Water phase infiltration expansion ratio- Oil Viscosity Curve

By calculating the nuclear magnetic results when the water displacement multiple of group 12-15 is 50PV and 1000PV, the remaining oil signal intensity in each pore radius at different crude oil viscosities can be obtained, and the oil displacement efficiency changes of each pore diameter can be calculated accordingly. It can be found, as shown in Fig.9, that for group 2mPa·s with low viscosity, the incremental oil displacement efficiency mainly comes from large pores with pore radius greater than 20um. For the medium and high viscosity group, the increment of displacement efficiency mainly comes from small holes with pore radius less than 10um.
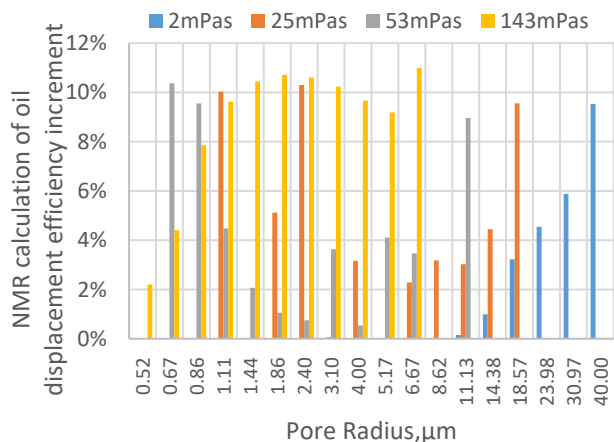

Fig. 9 Displacement efficiency increment of pore radius with different oil viscosity at 50PV-1000PV

4.3 The effect of permeability

By calculating the high multiple water flooding relative permeability curve of group 5-8, as shown in Fig.10, it can be found that with the increase of permeability, the isotonic point and wettability change little with the permeability. The residual oil saturation increases with the increase of permeability.
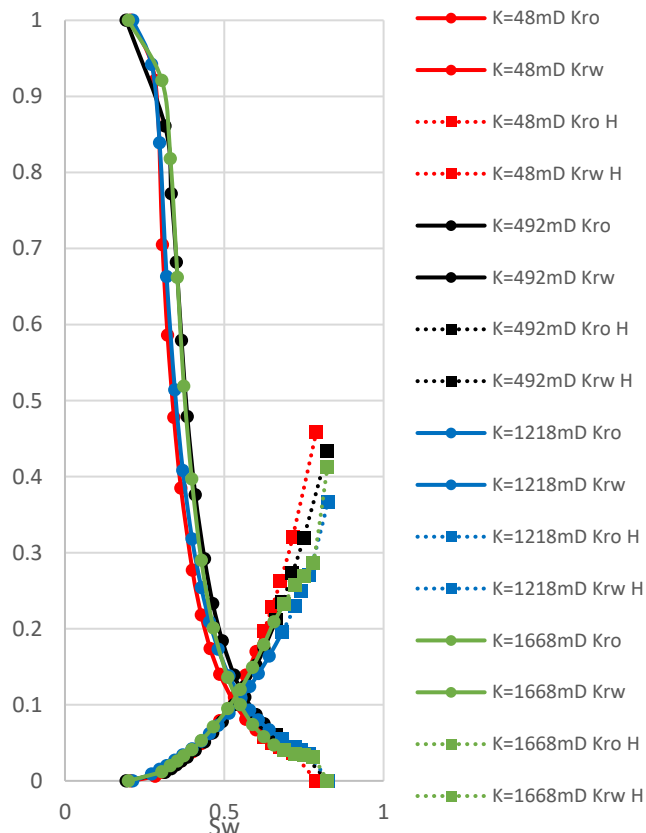

Fig. 10 Group 5-8 relative permeability curves of conventional and high-multiple water flooding with different permeabilities

By comparing the right shift ratio of residual oil and the expansion ratio of water phase infiltration when the water drive ratio is 1000PV and 50PV, as shown in Fig.11 and Fig.12, it can be found that with the increase of core permeability, the right shift ratio of residual oil in high water drive decreases from 1.26 to 1.20. With the increase of core permeability, the expansion ratio of water phase infiltration decreases from 2.33 to 1.77. The lower the permeability is, the higher the oil increase potential is.
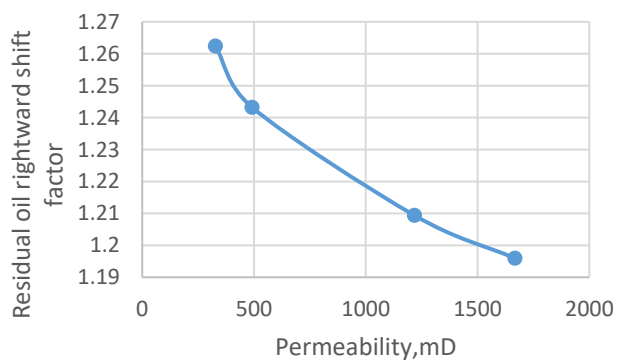

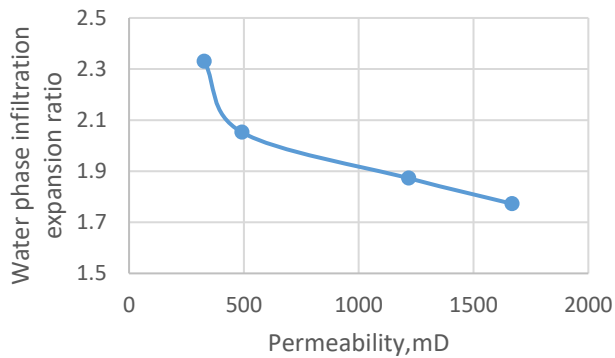*Fig. 11 Residual oil rightward shift factor- Permeability Curve*

Fig. 12 Water phase infiltration expansion ratio-Permeability Curve

By calculating the nuclear magnetic results of groups 12 and 16-18 when the water flooding multiple is 50PV and 1000PV, the remaining oil signal intensity in each pore radius at different permeability can be obtained, and the oil displacement efficiency changes at each pore diameter can be calculated accordingly. It can be found, as shown in Fig.13, that the oil displacement efficiency increment is the largest at the 23.98um pore radius scale for each average permeability group. For the reservoir with low permeability of 106mD, the increment of displacement efficiency of each pore radius is the largest, and the increment of 23.98um radius is the largest. For the hypertonic group 751mD, the increment of displacement efficiency mainly came from small hole 8.62um and large hole 40um, and the increment of medium hole was limited.
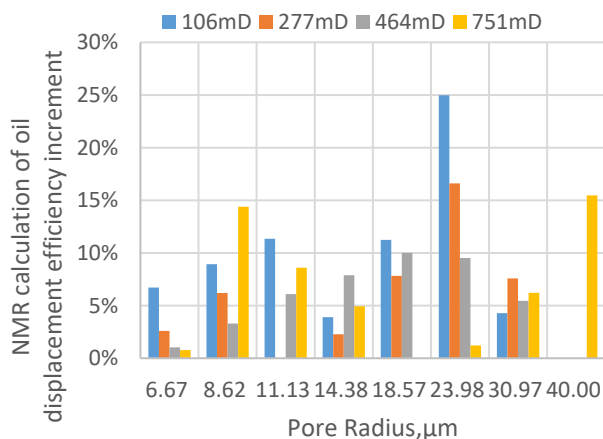
In order to reflect the actual flow velocity of fluid in the core, this paper uses capillary number to characterize the water flooding velocity, Nca=vμ/σ. According to core size and experimental displacement speed, capillary number under different displacement speed can be obtained, as shown in Table .2..

Table. 2 Conversion of Experiment water flooding speed and Capillary number

Experiment water flooding speed （mL/min）	Water viscosity （mPa·s）	Surface tension （mN/m）	*Capillary number*
0.05	1.0	10	1.88×10^{-7}
0.1	1.0	10	3.75×10^{-7}
0.5	1.0	10	1.88×10^{-6}
1.0	1.0	10	3.75×10^{-6}
2.0	1.0	10	7.50×10^{-6}

By calculating the high multiple water flooding relative permeability curve of group 9-11, as shown in Fig.14, it can be found that with the increase of displacement velocity, the isotonic point shifts to the right, and the wettability trend becomes stronger. With the increase of displacement speed, the residual oil saturation increases. With the increase of displacement velocity, the residual oil saturation corresponds to the increase of water phase relative permeability.
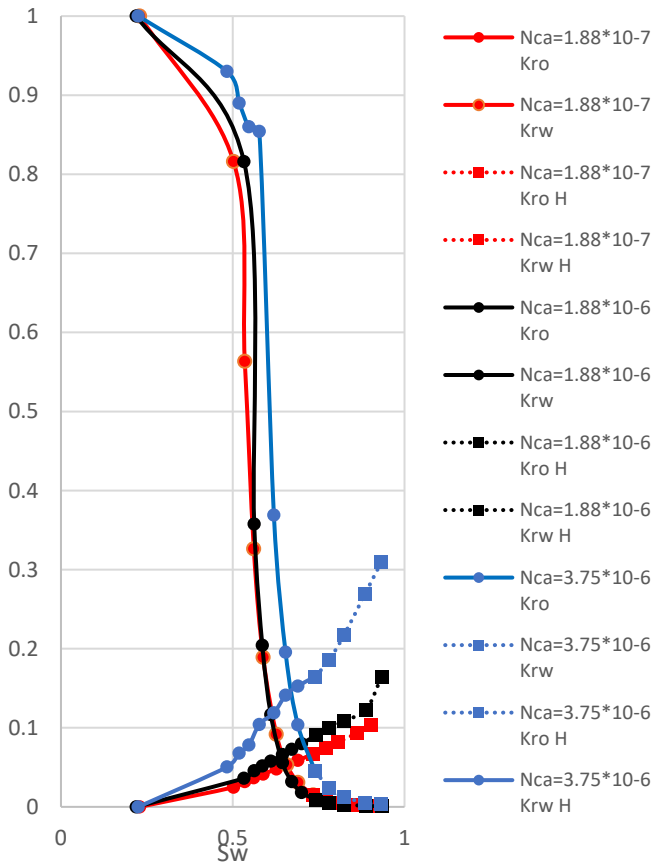

Fig. 13 Displacement efficiency increment of pore radius with different permeability at 50PV-1000PV

4.4 The effect of capillary number

Fig. 14 Group 9-11 relative permeability curves of conventional and high-multiple water flooding with different capillary numbers

Fig. 15 Residual oil rightward shift factor- Capillary Number Curve
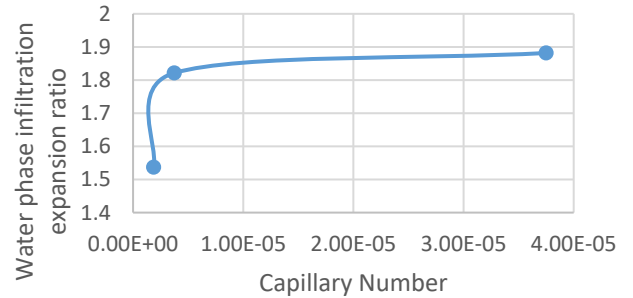
Fig. 16 Water phase infiltration expansion ratio- Capillary Number Curve

By comparing the right shift ratio of residual oil and the expansion ratio of water phase infiltration when the water drive ratio is 1000PV and 50PV, as shown in Fig.15 and Fig.16, it can be found that the right shift ratio of residual oil after high speed water drive increases with the increase of capillary number, from 1.23 to 1.26. The oil drive efficiency at high speed is greatly improved, and the oil drive efficiency is increased by 2.4% compared with that at low speed. After high-power water flooding, the expansion ratio of water phase infiltration increases with the increase of capillary number, from 1.54 to 1.88, and high-speed water flooding can improve water phase flow capacity. At high speed, there is more oil increase through high water flooding, while at low speed, there is less oil increase potential.
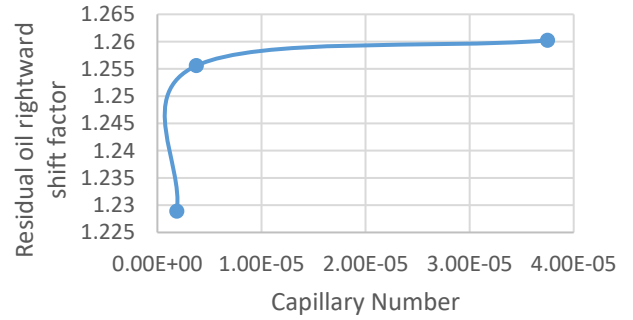
By calculating the nuclear magnetic results of groups 12 and 19-21 when the water flooding multiple is 50PV and 1000PV, the remaining oil signal intensity in each pore radius at different capillary numbers can be obtained, and the oil displacement efficiency changes of each pore diameter can be calculated accordingly. It can be found, as shown in Fig.17, that from the point of view of the use degree of pore throat, the oil displacement efficiency of 37.18um pore size is limited by high water flooding. At low speed, the displacement efficiency of each aperture increases, and the increment of small aperture is more for 8.62um. The increment of displacement efficiency under high speed condition mainly comes from the large and medium aperture of 27.75um.
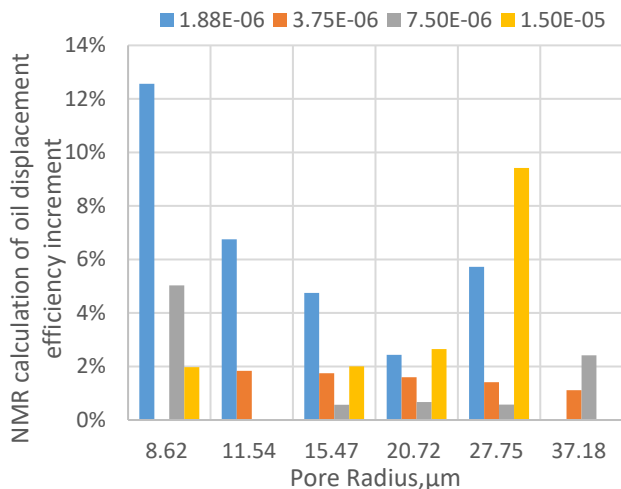
Fig. 17 Displacement efficiency increment of pore radius with different capillary number at 50PV-1000PV

5. CONCLUSIONS

1. Oil displacement efficiency increases with the increase of water displacement multiple. The larger the water displacement multiple is, the smaller the increase of oil displacement efficiency is; The oil phases in different pore radius are used, and the displacement efficiency of large holes is higher than that of small holes.

2. With the increase of oil viscosity, the right shift ratio of residual oil in high-power water drive increases, and is 1.11 at low viscosity and 1.29 at high viscosity. With the increase of oil viscosity, the expansion ratio of water phase in high multiple water flooding increases, and is 1.07 at low viscosity and 2.28 at high viscosity. The increment of oil displacement efficiency in low-viscosity group is mainly from large pores with pore radius greater than 20um, and the increment of oil displacement efficiency in medium-high viscosity group is mainly from small pores with pore radius less than 10um.

3. With the increase of core permeability, the right-shifting ratio of residual oil and the water-phase expansion ratio of high multiple water flooding decrease, and the lower the permeability, the more oil increase potential of high multiple water flooding. The oil displacement efficiency of each pore radius in the low permeability group increased, and the increment of oil displacement efficiency in the high permeability group mainly came from the small hole about 8.62um.

4. After high multiple water flooding, the right-shift ratio of residual oil increases with the increase of capillary number, and the oil displacement efficiency is greatly improved at high speed, and the expansion ratio of water phase infiltration increases with the increase of capillary number after high multiple water flooding. High-speed water flooding can improve the water phase flow capacity, and the oil increase potential is relatively low at low speed. At low speed, the displacement efficiency of each aperture increases, and the increment of small aperture is more for 8.62um. The increment of displacement efficiency under high speed condition mainly comes from the large and medium aperture of 27.75um.

REFERENCE

[1] Xu J, Guo C, Jiang R, et al.Study on relative permeability characteristics affected by displacement pressure gradient: Experimental study and numerical simulation. Fuel. 2016,163:314-323.

[2] Zhang L, Tong J, Xiong Y, et al.Effect of temperature on the oil–water relative permeability for sandstone reservoirs. International Journal of Heat and Mass Transfer. 2017,105:535-548.

[3] Guo C, Wang X, Wang H, et al.Effect of pore structure on displacement efficiency and oil-cluster morphology by using micro computed tomography (μCT) technique. Fuel. 2018,230:430-439.

[4] Miao T, Long Z, Chen A, et al.Analysis of permeabilities for slug flow in fractal porous media. International Communications in Heat and Mass Transfer. 2017,88:194-202.

[5] Esmaeili S, Sarma H, Harding T, et al.Review of the effect of temperature on oil-water relative permeability in porous rocks of oil reservoirs. Fuel. 2019,237:91-116.

[6] Esmaeili S, Sarma H, Harding T, et al.Correlations for effect of temperature on oil/water relative permeability in clastic reservoirs. Fuel. 2019,246:93-103.

[7] Esmaeili S, Sarma H, Harding T, et al.A data-driven model for predicting the effect of temperature on oil-water relative permeability. Fuel. 2019,236:264-277.

[8] Doranehgard M H, Siavashi M.The effect of temperature dependent relative   permeability on heavy oil recovery during hot water injection process using streamline-based simulation. Applied Thermal Engineering. 2018,129:106-116.

[9] Krause M H, Benson S M.Accurate determination of characteristic relative permeability curves. Advances in Water Resources. 2015,83:376-388.

[10] Lai B, Miskimins J L.A new technique for accurately measuring two-phase relative permeability under non-Darcy flow conditions. Journal of Petroleum Science and Engineering. 2015,127:398-408.

[11] Ge Y, Li S, Qu K.A Novel Empirical Equation for Relative Permeability in Low Permeability Reservoirs.Chinese Journal of Chemical Engineering. 2014,22(11-12):1274-1278.

[12] Zhang D, Papadikis K, Gu S.A lattice Boltzmann study on the impact of the geometrical properties of porous media on the

steady state relative permeabilities on two-phase immiscible flows. Advances in Water Resources. 2016,95:61-79.

[13] Alpak F O, Berg S, Zacharoudiou I.Prediction of fluid topology and relative permeability in imbibition in sandstone rock by direct numerical simulation. Advances in Water Resources. 2018,122:49-59.

[14] Shi Y, Tang G H.Relative permeability of two-phase flow in three-dimensional porous media using the lattice Boltzmann method. International Journal of Heat and Fluid Flow. 2018,73:101-113.

[15] Aghabozorgi S, Sohrabi M.A comparative study of predictive models for imbibition relative permeability and trapped non-wetting phase saturation. Journal of Natural Gas Science and Engineering. 2018,52:325-333.

[16] Zhang T, Li X, Sun Z, et al.An analytical model for relative permeability in water-wet nanoporous media.Chemical Engineering Science. 2017,174:1-12.

[17] Torabi F, Mosavat N, Zarivnyy O.Predicting heavy oil/water relative permeability using
modified Corey-based correlations. Fuel. 2016,163:196-204.

[18] CHEN Ke, HE Wei, ZHANG Xudong, et al. Mechanism and application of high-power waterflooding in a sandstone reservoir with side-bottom water in a certain area of the Bohai Sea. Petrochemical Industry Application,2021,40(2):25-28,49.

[19] SUN Changwei, CHENG Jia, ZHAO Mingyue et al. Phase－permeability transfer method in digital simulation of high－power waterflooding reservoir——Taking marine XJ oilfield as an example. Petroleum Geology and Engineering,2023,37(01):66-70.